2023 IEEE International Conference on Robotics and Automation (ICRA 2023)
May 29 - June 2, 2023. London, UK

Identification of a Generalized Base Inertial Parameter Set of Robotic Manipulators Considering Mounting Configurations

Mario Tröbinger*, Abdeldjallil Naceri, Xiao Chen, Hamid Sadeghian◇, and Sami Haddadin

***Abstract*— Identifying the inertial parameters of real robotic manipulators is a fundamental step towards realistic modeling and better controller performances, which is crucial for safe human-robot interaction. Our work introduces a novel framework for identifying a generalized set of base inertial parameters of a serial link manipulator. This framework is designed to be adaptable to accommodate any new mounting configuration of the robot. Our theoretical analysis highlights the influence of the robot's mounting configuration on the emergence of new parameters that cannot be identified through the conventional vertical base-axis mounting approach studied previously. To validate our proposed framework, we carried out two main experiments: the first involved simulation to establish the feasibility of our concept, and in the second, our framework was employed on a Franka Emika Robot in a real-world scenario to demonstrate and validate our approach. Our simulation results confirmed the feasibility of our proposed framework, while our real-world experiment successfully identified the generalized base inertial parameter set and validated its applicability to a new robot mounting configuration.**

I. INTRODUCTION

Identifying the robot dynamics has been the subject of research over the past three decades (see e.g., [1], [2]) as the accuracy of dynamic models is critical for many robotic applications such as model-based control, simulation, learning, and physical interaction. Due to its importance, methods for identifying system inertial parameters have been developed for several types of robots, e.g., humanoid robots [3]–[5], industrial robots [6], [7] and light-weight research robots [8], [9]. There are several methods to estimate these inertial parameters, e.g., by generating inertial parameters via computer-aided design (CAD) data [10]. However, due to the existence of motors, wires, reducers, etc., this method lacks accuracy and is used less and less. A more standard approach is the identification of inertial parameters based on rigorous analyses of joint movements and torques, such as inverse dynamic identification models with ordinary least-squares estimation (IDIM-OLS) [1], [11]. This method assumes that joint torques and the inertial parameters of a robot are linearly correlated. In addition, there are two other approaches that are variants of IDIM-OLS, namely weighted least-squares (IDIM-WLS) and total least-squares (IDIM-TLS). These methods are highly dependent on the filter methods used and require good excitation trajectories [7], [12], [13]. Based on successful application to several prototypes and industrial robots [6], [7], [14], IDIM-WLS is chosen as the identification method in this paper.

The identification of the inertial parameters of industrial and lightweight research robots is mostly done in their default configuration where the first joint axis of the robot is parallel to the gravitational axis (defined as *"V-BAM": Vertical Base-Axis Mount* in the rest of the paper). Other mounting configurations require a change in the orientation of the robot base, which will likely affect the identifiable set of inertial parameters [11]. Therefore, a mounting configuration for the identification procedure that contains a generic set of inertial parameters would be beneficial. That set can be applied to model the dynamics for any new robot mounting configuration.

In this study, we aim to demonstrate that a wall-mounted robot with the first joint axis perpendicular to the gravitational axis (*"H-BAM": Horizontal Base-Axis Mount*) will show new parameters to be identified that were not experienced (were unidentifiable) during *V-BAM* condition. We hypothesize that the identified inertial parameters in the *H-BAM* configuration are more complete and can be used for other mounting configurations. To the best of the authors' knowledge, this is the first study addressing the effects of other mounting configurations of the robot base on the identification of base inertial parameters. Hereby, we contribute to fundamental knowledge in identifying inertial parameters that is essential for developing more complex synergetic robotic systems, such as humanoids or mobile systems [15].

A. Related Work

Previous research on the identification of inertial parameters of commercial lightweight robotic manipulators was mainly conducted in *V-BAM* configuration. The authors of [14] identified the inertial parameters of a rigid-link model of the KUKA LBR iiwa 14 R820 robot. Moreover, in [8] the parameters that characterize the dynamics of the Franka Emika Robot [16] were identified. The authors of [17] proposed a method for estimating the inertial parameters using the torque separation technique and applied it to two robotic manipulators: Franka Emika Robot and eZRO.

Finally, a very recent work tackled the same question of estimating the inertial parameters of robots in different mounting configurations [18]. However, the latter work presented a framework where the identified parameters or model depends crucially on how precise the gravity vector is identified (i.e., relative orientation to the base frame). In other words, this represents a strong assumption, thus, the base parameters are non-generic and can be applied only to the same robot mounting configuration used during the identification proce-

All authors are with Munich School of Robotics and Machine Intelligence, Technical University of Munich, 80797 Munich, Germany ◇and Faculty of Engineering, University of Isfahan, 8174673441 Isfahan, Iran.
*Corresponding Author: mario.troebinger@tum.de

dure.
The aim of these studies was to determine the inertial parameters of the robot in *V-BAM* configuration with a specific level of precision. However, these parameters are not suitable for modeling the dynamics of a robot in *H-BAM* configuration or a robot with a generic mounting angle, unless the center of mass (COM) of the first two robot joints is aligned in such a way as to eliminate any momentum around the first joint axis in *H-BAM* configuration. The latter tends to be a strong assumption, especially regarding unidentifiable parameters (e.g., COM of the first robot link) as we demonstrate later in this paper. Our paper goes beyond the state-of-the-art considering the following issues:

- Demonstrating in theory and simulation that the inertial parameters of robots mounted in *H-BAM* configuration can be used for a robot mounted in *V-BAM* configuration and not vice-versa,
- Identifying a generalized robot base parameter set of a Franka Emika Robot mounted in *H-BAM* configuration in a real robot experiment,
- Demonstrating and validating the identified inertial parameters on a robot mounted in both *H-BAM* and *V-BAM* configurations respectively.

II. METHODOLOGY

In this section, we summarize the robot dynamics, propose our methodology of defining generalized robot base parameters that are independent of the robot mounting configuration, and outline the identification procedure.
For the modeling and identification procedure, it is assumed that the first robot joint is a revolute joint and the axis of the second joint is not parallel to the axis of the first one: ${}^0\boldsymbol{j}_1 \nparallel {}^0\boldsymbol{j}_2$.

A. Modeling

1) Robot Dynamic Model: The robot arm is considered as an open kinematic chain of $n+1$ rigid bodies and n rigid joints. The generalized coordinates $\boldsymbol{q} \in \mathbb{R}^n$ represent the configuration of the n joint angles. The dynamic model of the robot is

$$\boldsymbol{M}(\boldsymbol{q})\ddot{\boldsymbol{q}} + \boldsymbol{C}(\boldsymbol{q},\dot{\boldsymbol{q}})\dot{\boldsymbol{q}} + \boldsymbol{g}(\boldsymbol{q}) = \boldsymbol{\tau} - \boldsymbol{\tau}_f, \tag{1}$$

where $\boldsymbol{M}(\boldsymbol{q}) \in \mathbb{R}^{n\times n}$ denotes the inertia matrix, $\boldsymbol{C}(\boldsymbol{q},\dot{\boldsymbol{q}})\dot{\boldsymbol{q}} \in \mathbb{R}^n$ the centrifugal and Coriolis torque, $\boldsymbol{g}(\boldsymbol{q}) \in \mathbb{R}^n$ the gravity torque and $\boldsymbol{\tau} \in \mathbb{R}^n$ the actuation torque. Moreover, $\boldsymbol{\tau}_f \in \mathbb{R}^n$ represents the dissipative torque, mostly due to joint friction. We consider only viscous and Coulomb friction, which results in the following friction model,

$$\boldsymbol{\tau}_f = \boldsymbol{F}_v\dot{\boldsymbol{q}} + \boldsymbol{F}_c\tanh(100\dot{\boldsymbol{q}}), \tag{2}$$

where $\boldsymbol{F}_v \in \mathbb{R}^{n\times n}$ and $\boldsymbol{F}_c \in \mathbb{R}^{n\times n}$ denote the diagonal matrices of the viscous and Coulomb friction coefficients, respectively. Using the hyperbolic function $\tanh(\cdot)$ instead of the signum function $\mathrm{sign}(\cdot)$ ensures the continuity of the Coulomb friction torque during change in rotation direction. In our approach, we go beyond the current state-of-the-art of identification models and substitute the gravitational acceleration vector into the Lagrange or Newton-Euler formulation. The gravitational acceleration vector expressed in robot base frame ${}^0\boldsymbol{a}_g \in \mathbb{R}^3$ is parameterized using spherical coordinates:

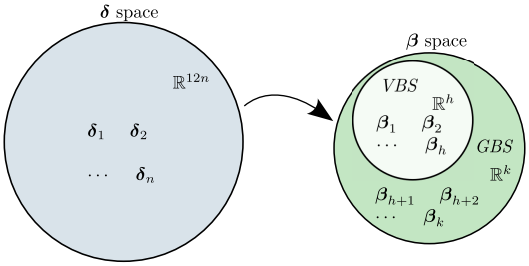

Fig. 1: Transformation from the standard $\boldsymbol{\delta}$ to the base $\boldsymbol{\beta}$ inertial parameter space. The *VBS* (e.g. identified in *V-BAM* configuration) is a subset of the *GBS* (e.g. identified in *H-BAM* configuration).

$${}^0\boldsymbol{a}_g = g \begin{bmatrix} \sin(\rho)\cos(\phi) \\ \sin(\rho)\sin(\phi) \\ \cos(\rho) \end{bmatrix}, \tag{3}$$

where $g = 9.81 m/s^2$ denotes the gravitational acceleration and ρ, ϕ are the spherical parameterization variables.
The choice of modified Denavit-Hartenberg (DH) frames attached to each link allows a formulation of the dynamic model which is linear with respect to the standard inertial parameters $\boldsymbol{\delta}_i \in \mathbb{R}^{12}$, $i = 1, \cdots, n$,

$$\underbrace{\begin{bmatrix} \tau_1 \\ \tau_2 \\ \vdots \\ \tau_n \end{bmatrix}}_{\boldsymbol{\tau}} = \underbrace{\begin{bmatrix} \boldsymbol{y}_{11}^\top & \boldsymbol{y}_{12}^\top & \cdots & \boldsymbol{y}_{1n}^\top \\ 0 & \boldsymbol{y}_{22}^\top & \cdots & \boldsymbol{y}_{2n}^\top \\ \vdots & \vdots & \ddots & \vdots \\ 0 & 0 & \cdots & \boldsymbol{y}_{nn}^\top \end{bmatrix}}_{\boldsymbol{Y}(\boldsymbol{q},\dot{\boldsymbol{q}},\ddot{\boldsymbol{q}},\rho,\phi)} \underbrace{\begin{bmatrix} \boldsymbol{\delta}_1 \\ \boldsymbol{\delta}_2 \\ \vdots \\ \boldsymbol{\delta}_n \end{bmatrix}}_{\delta}, \tag{4}$$

$$\begin{aligned} \boldsymbol{\delta}_i = [&L_{xx,i}\, L_{xy,i}\, L_{xz,i}\, L_{yy,i}\, L_{yz,i}\, L_{zz,i}\ \cdots \\ &\cdots l_{x,i}\, l_{y,i}\, l_{z,i}\, m_i\, f_{v,i}\, f_{c,i}]^\top, \end{aligned} \tag{5}$$

where $\boldsymbol{Y}(\boldsymbol{q},\dot{\boldsymbol{q}},\ddot{\boldsymbol{q}},\rho,\phi) \in \mathbb{R}^{n\times 12n}$ denotes the observation matrix (regressor matrix) of the standard inertial parameters. Note that, this matrix is not only a function of the generalized joint coordinates $\boldsymbol{q}, \dot{\boldsymbol{q}}$ and $\ddot{\boldsymbol{q}}$ but also depends on the gravitational acceleration parameters ρ and ϕ (see Equation (3)). Moreover, for the link i, $L_{xx,i}, L_{xy,i}, L_{xz,i}, L_{yy,i}, L_{yz,i}, L_{zz,i}$ are the components of the symmetric inertia matrix expressed in joint frame i, m_i is the mass, and $f_{v,i}, f_{c,i}$ are the viscous and the Coulomb friction coefficients, respectively. $l_{x,i}, l_{y,i}, l_{z,i}$ are the components of the first moments of mass,

$$\begin{bmatrix} l_{x,i} & l_{y,i} & l_{z,i} \end{bmatrix}^\mathsf{T} = m_i \boldsymbol{r}_{c,i}, \tag{6}$$

where $\boldsymbol{r}_{c,i} \in \mathbb{R}^3$ is the COM relative to the link frame i.

2) Reduction to Generalized Base Parameters: Only a subset of the standard inertial parameters is necessary for modeling the robot dynamics. Moreover, some of those are not separately identifiable by regression methods. To obtain this set of parameters, a process of regrouping and combining the identifiable standard parameters is required, as described in [2]. This minimum parameter set is called the robot's base inertial parameters $\boldsymbol{\beta} \in \mathbb{R}^m$ [2]. The dynamics of the robotic manipulator can then be written as,

$$\boldsymbol{\tau} = \boldsymbol{Y}_b(\boldsymbol{q},\dot{\boldsymbol{q}},\ddot{\boldsymbol{q}})\boldsymbol{\beta}, \tag{7}$$

where $\boldsymbol{Y}_b(\boldsymbol{q}, \dot{\boldsymbol{q}}, \ddot{\boldsymbol{q}}) \in \mathbb{R}^{n \times m}$ denotes the regressor matrix of the base inertial parameters.

The number of identifiable robot base parameters m depends not only on the robot kinematic structure, i.e. DH parameters, but also on its mounting configuration [2]. The robot's kinematic structure is given by the manufacturers, whereas the mounting configuration for any identification procedure is modifiable. If the robot mounting is chosen such that the gravitational acceleration vector is not parallel to the axis of the first joint ${}^0\boldsymbol{a}_g \nparallel {}^0\boldsymbol{j}_1$ (e.g. *H-BAM* robot configuration), a maximum number of k base inertial parameters can be identified. We define them as the *Generalized robot Base parameter Set* (*GBS*). While choosing the gravitational acceleration vector parallel to the axis of the first joint ${}^0\boldsymbol{a}_g \parallel {}^0\boldsymbol{j}_1$ (e.g. *V-BAM* robot configuration), only a minimum number of h base inertial parameters can be identified. We define them as the *V-BAM robot Base parameter Set* (*VBS*). Furthermore, the *VBS* is a subset of the *GBS*, see Fig. 1. Therefore, the *GBS* can be used to model the robot dynamics for any new static robot mounting configuration, including the *V-BAM* robot configuration, but not vice versa. This effect can be shown by the derivation of the kinetic and potential energy of the manipulator according to standard inertial parameters of the first two links [2].

Table I shows a comparison between the *GBS* and *VBS* of a 7-DOF serial link manipulator (e.g. Franka Emika Robot, Kuka LWR). By choosing a robot mounting configuration in which the gravitational acceleration vector is not parallel to the first joint axis, thus, the base parameter set size increases. Specifically, the new base parameters β_{58} and β_{59} can be additionally identified. These two extra parameters are restricted to the first two links of the robot [2] and solely influence the computation of the torque τ_1 at the first joint in the following manner[1],

$$\tau_1 = \tau_1^* + \sin(\rho) g \begin{bmatrix} \cos(\phi)\sin(q_1) - \sin(\phi)\cos(q_1) \\ \cos(\phi)\cos(q_1) + \sin(\phi)\sin(q_1) \end{bmatrix}^\mathsf{T} \begin{bmatrix} \beta_{58} \\ \beta_{59} \end{bmatrix} \quad (8)$$

If and only if the gravitational acceleration vector is parallel to the axis of the first joint ${}^0\boldsymbol{a}_g \parallel {}^0\boldsymbol{j}_1$ ($\rho = k\pi$, $\forall k \in \mathbb{N}$ – e.g., *V-BAM* configuration) the term associated with the two additional base parameters will disappear and will not affect the robot's dynamics. This theoretical example confirms our hypothesis that the inertial parameters identified in the *H-BAM* configuration are more general and can be used to model the dynamics of any new robot mounting configuration. In contrast, the base parameters identified in the *V-BAM* configuration can only be applied to a mounting configuration where the gravitational acceleration is parallel to the axis of the first joint.

B. Identification Procedure

1) Parameter Estimation (IDIM-WLS): The parameter estimation is based on the measurements of the actuation torques and the joint angles. The joint velocities and accelerations are calculated from the measured joint angles. p measurements along the optimized excitation trajectory are taken. The over-determined linear system is

$$\underbrace{\begin{bmatrix} \boldsymbol{\tau}(1) \\ \boldsymbol{\tau}(2) \\ \vdots \\ \boldsymbol{\tau}(p) \end{bmatrix}}_{\bar{\boldsymbol{\tau}}} = \underbrace{\begin{bmatrix} \boldsymbol{Y}_b(\boldsymbol{q}(1), \dot{\boldsymbol{q}}(1), \ddot{\boldsymbol{q}}(1)) \\ \boldsymbol{Y}_b(\boldsymbol{q}(2), \dot{\boldsymbol{q}}(2), \ddot{\boldsymbol{q}}(2)) \\ \vdots \\ \boldsymbol{Y}_b(\boldsymbol{q}(p), \dot{\boldsymbol{q}}(p), \ddot{\boldsymbol{q}}(p)) \end{bmatrix}}_{\bar{\boldsymbol{Y}}_b} \boldsymbol{\beta} + \underbrace{\begin{bmatrix} \boldsymbol{\epsilon}(1) \\ \boldsymbol{\epsilon}(2) \\ \vdots \\ \boldsymbol{\epsilon}(p) \end{bmatrix}}_{\bar{\boldsymbol{\epsilon}}}, \quad (9)$$

where $\boldsymbol{\epsilon}(j) \in \mathbb{R}^n$ is the vector of errors of the j^{th} measurement. Assuming that the noise level of the measured joint angles is much smaller than the noise level of the measured actuation torques allows using the weighted least-square (WLS) estimation method instead of maximum-likelihood estimation [13]. Moreover, $\boldsymbol{\epsilon}$ is assumed to have a zero mean, being serially uncorrelated and heteroscedastic. That results in a diagonal covariance matrix of the measured actuator torques [1]. The WLS solution is then given by,

$$\begin{aligned} \hat{\boldsymbol{\beta}} &= (\bar{\boldsymbol{Y}}_b^\top \boldsymbol{\Sigma}^{-1} \bar{\boldsymbol{Y}}_b)^{-1} \bar{\boldsymbol{Y}}_b^\top \boldsymbol{\Sigma}^{-1} \bar{\boldsymbol{\tau}} \\ &= (\boldsymbol{\Sigma}^{-0.5} \bar{\boldsymbol{Y}}_b)^+ \boldsymbol{\Sigma}^{-0.5} \bar{\boldsymbol{\tau}}\,, \end{aligned} \quad (10)$$

where $\boldsymbol{\Sigma} \in \mathbb{R}^{np \times np}$ denotes the stacked matrix of the diagonal covariance matrices of p measurements. The condition number of the stacked matrix $\bar{\boldsymbol{Y}}_b$ in equation (9) measures the sensitivity of the least squares estimates of $\hat{\boldsymbol{\beta}}$. Therefore, it is an appropriate criterion for designing trajectories, as minimizing the condition number can improve the robustness of the least squares estimates.

2) Optimal Excitation Trajectories: The smaller the condition number, the better the estimates. Thus, the minimum of the condition number of the normalized matrix $\boldsymbol{\Sigma}^{-0.5}\bar{\boldsymbol{Y}}_b$ is used as an optimization cost function for generating optimal excitation trajectories [13],

$$\min_{a_{i,k}, b_{i,k}} \operatorname{cond}\left(\boldsymbol{\Sigma}^{-0.5}\bar{\boldsymbol{Y}}_b\right). \quad (11)$$

Various methods can be used to parameterize the excitation trajectories, including B-splines [12], combined Fourier series and polynomial functions [19], and others. However, it has been demonstrated by [14] and confirmed by our own experimental results that finite Fourier series [13] is the most suitable method, as they produce the lowest condition number. The joint trajectories can be expressed as follows,

$$\begin{aligned} q_i(t) &= q_{i0} + \sum_{k=1}^{N} (a_{i,k}\sin(k\omega_f t) + b_{i,k}\cos(k\omega_f t)) \\ \dot{q}_i(t) &= \sum_{k=1}^{N} (a_{i,k} k\omega_f \cos(k\omega_f t) - b_{i,k} k\omega_f \sin(k\omega_f t)) \\ \ddot{q}_i(t) &= \sum_{k=1}^{N} (-a_{i,k} k^2\omega_f^2 \sin(k\omega_f t) - b_{i,k} k^2\omega_f^2 \cos(k\omega_f t)), \end{aligned} \quad (12)$$

where q_{i0} denotes the offset of the position trajectory, ω_f the fundamental pulsation of the Fourier series with period $T_f = \frac{2\pi}{\omega_f}$ and t the time. The amplitudes of the Fourier series $a_{i,k}$ and $b_{i,k}$ are the parameters of the non-linear optimization problem, which has $2 \times N$ degrees of freedom. For the experiments in this paper, N is set to 5, T_f is set to

[1] Please note: $\boldsymbol{\tau}_1^*$ results from parameters $\beta_1 \cdots \beta_{57}$ which are independent of the robot mounting configuration in contrast to β_{58} and β_{59} that are configuration dependent.

Nr.	Math. Symbol	*GBS*	*VBS*
β_1	$L_{zzR,1}$	$L_{zz,1} + L_{yy,2}$	$L_{zz,1} + L_{yy,2}$
β_2	$L_{xxR,2}$	$L_{xx,2} + L_{yy,3} - L_{yy,2} + k_{2,1}(m_4 + m_5 + m_6 + m_7) + + k_{2,2}m_3 + k_{2,3}l_{z,3}$	$L_{xx,2} + L_{yy,3} - L_{yy,2} + k_{2,1}(m_4 + m_5 + m_6 + m_7) + + k_{2,2}m_3 + k_{2,3}l_{z,3}$
$\vdots$	$\vdots$	$\vdots$	$\vdots$
β_{57}	$f_{cR,7}$	$f_{c,7}$	$f_{c,7}$
β_{58}	$l_{xR,1}$	$l_{x,1}$	-
β_{59}	$l_{yR,1}$	$l_{y,1} + l_{z,2}$	-

TABLE I: Comparison of *GBS* and *VBS* for a 7-DOF robotic manipulator (Fig. 5). Column two defines the base parameters' mathematical expressions. Constant variables $k_{i,j}$ (joint i) are defined by robot kinematics. Grey rows are additional base inertial parameters identifiable only if ${}^0\boldsymbol{a}_g \nparallel {}^0\boldsymbol{j}_1$ during identification.

$10s$, and the sampling frequency is set to $1000Hz$.
To ensure that the trajectory starts and ends in a predefined configuration q_{i0} with zero initial joint velocities and accelerations, the following conditions have to be fulfilled,

$$\sum_{k=1}^{5} b_{i,k} = 0, \ \sum_{k=1}^{5} a_{i,k} = 0, \ \sum_{k=1}^{5} b_{i,k} k^2 = 0 \ . \tag{13}$$

To avoid collisions with both the environment and the robot itself, constraints must be placed on the end-effector position, denoted by $\boldsymbol{x}_{ee} \in \mathbb{R}^3$ [12]. The workspace is limited to a cubic box surrounding the robot arm to prevent collisions with the environment, while the self-collision constraint is defined by a sphere with radius r_s around the robot base. The motion constraints are as follows,

$$\boldsymbol{x}_{min} < \boldsymbol{x}_{ee} < \boldsymbol{x}_{max}, \ r_s < |\boldsymbol{x}_{ee}| \tag{14}$$

Furthermore, it is necessary to consider the joint and motor limits of the manipulator,

$$c_{min,i} \leq c_i \leq c_{max,i} \tag{15}$$

where c_i stands for $p \subset \{q_i, \dot{q}_i, \ddot{q}_i, \tau_i\}$.

3) Data Acquisition and Filtering Method: The IDIM-WLS approach strongly depends on the accurate filtering of measurements. Noisy or incorrectly filtered signals can introduce bias in the estimates [1]. To address this issue, the measured data $\boldsymbol{q}$ and $\boldsymbol{\tau}$ are first averaged over 10 excitation periods. The resulting averaged joint angle measurements $\boldsymbol{q}$ are then filtered in the forward and reverse directions offline, using a noncausal zero-phase digital IIR lowpass Butterworth filter of order 20 and a cutoff frequency of $2Hz$. The derivatives $\dot{\boldsymbol{q}}$ and $\ddot{\boldsymbol{q}}$ are calculated using a central difference algorithm applied to the filtered joint position signals, without any phase shift.
Furthermore, a parallel decimation procedure can be applied to the measured joint torques to eliminate force/torque ripples. This procedure involves lowpass filtering and resampling the signals at a lower rate, keeping one sample over n_d [20].

$$n_d = \frac{2\pi 0.8 f_m}{\omega_{fp}} \ , \qquad \omega_{fp} > 2\omega_{dyn} \ , \tag{16}$$

where f_m denotes the measurement frequency and ω_{dyn} the maximum robot bandwidth. The given rule of thumb for the cutoff frequency ω_{fp} in Equation (16) allows to keep useful signals in the filter bandwidth [1].

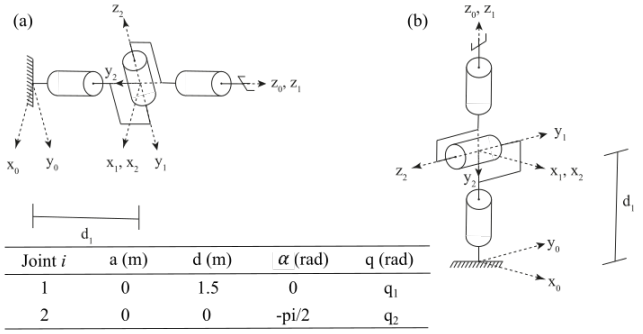

Fig. 2: Modified DH parameters and robot structure of the simulated 2-DOF robot in (a) *H-BAM* and (b) *V-BAM* configuration.

III. EXPERIMENTAL RESULTS AND VALIDATION

In this section, we demonstrate the generalizability of the proposed *GBS* framework for robot parameter identification to new mounting configurations. We also discuss the limitations of identifying the robot in *V-BAM* configuration. To validate our approach, we conduct experiments on both a simulated 2-DOF robot and a real Franka Emika Robot.
Specifically, we identify the *GBS* using a *H-BAM* robot configuration, where the gravitational acceleration vector is perpendicular to the axis of the first joint (${}^0\boldsymbol{a}_g \perp {}^0\boldsymbol{j}_1$).

A. Simulation Experiment: 2-DOF Robot Model

Assuming that the first robot joint is a revolute joint and ${}^0\boldsymbol{j}_1 \nparallel {}^0\boldsymbol{j}_2$, the extended set of identifiable inertial parameters in the *H-BAM* configuration is restricted to the first two robot links [2]. Therefore, simulation experiments are conducted on a 2-DOF robot (see Fig. 2). To highlight the influence of the robot mounting on the base inertial parameter identification problem and avoid any bias in the estimates, neither friction nor signal noise is modeled.
The base inertial parameters for the *H-BAM* and *V-BAM* robot configurations have been identified and are used to model the robot dynamics for both configurations.

Robot Description: To demonstrate the effect of the robot mounting configuration, the centers of mass for both joints have been chosen in such a way that they are not aligned with the axis of the first robot joint.

Estimation Procedure: The excitation trajectories of the robot are designed with the method discussed in section II-B.2. Assuming zero friction and noise, the relative residual error of the estimates is equal to zero.

Choosing a *V-BAM* robot configuration, where the gravitational acceleration vector is parallel to the axis of the first

Base Parameters	Regrouping of Standard Par.	*H-BAM* Model	*V-BAM* Model
$L_{zzR,1}$	$L_{zz,1} + L_{yy,2}$	0.320	0.320
$l_{xR,1}$	$l_{x,1}$	0.800	–
$l_{yR,1}$	$l_{y,1} + l_{z,2}$	1.100	–
$L_{xxR,2}$	$L_{xx,2} + L_{yy,2}$	1.590	1.590
$L_{xyR,2}$	$L_{xy,2}$	0.210	0.210
$L_{xzR,2}$	$L_{xz,2}$	−0.030	−0.030
$L_{yzR,2}$	$L_{yz,2}$	0.210	0.210
$L_{zzR,2}$	$L_{zz,2}$	1.660	1.660
$l_{xR,2}$	$l_{x,2}$	0.300	0.300
$l_{yR,2}$	$l_{y,2}$	−2.100	−2.100

TABLE II: Identified base inertial parameters of the simulated 2-DOF robot in *H-BAM* and *V-BAM* configuration.

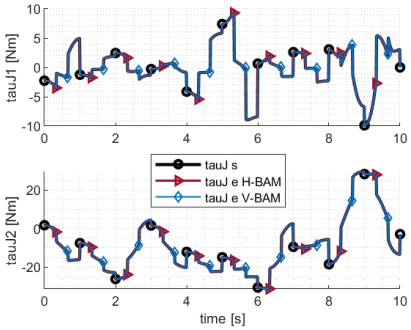

Fig. 3: Joint torque validation of the 2-DOF manipulator in *V-BAM* configuration (see Fig. 2(b)) using a random joint trajectory. $tauJ\ s$ denotes the simulated joint torque, $tauJ\ e\ H\text{-}BAM$ the torque modeled with the identified *H-BAM* base parameters and $tauJ\ e\ V\text{-}BAM$ the torque modeled with the identified *V-BAM* base parameters (see Table II).

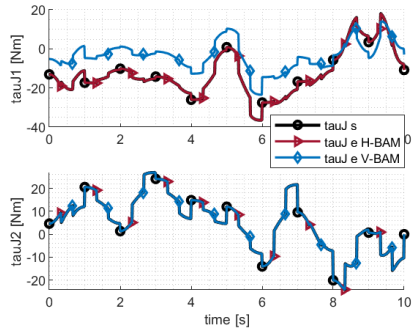

Fig. 4: Joint torque validation of a 2-DOF manipulator in *H-BAM* configuration (Fig. 2(a)) using a random joint trajectory. The root-mean-square (RMS) error of $tauJ1$ between measured/simulated torque and the modeled torque based on estimated parameters in *V-BAM* configuration is $10.9Nm$.

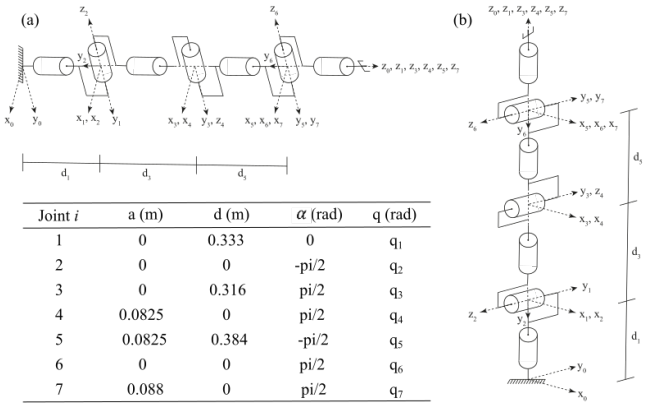

Joint *i*	a (m)	d (m)	α (rad)	q (rad)
1	0	0.333	0	q_1
2	0	0	-pi/2	q_2
3	0	0.316	pi/2	q_3
4	0.0825	0	pi/2	q_4
5	0.0825	0.384	-pi/2	q_5
6	0	0	pi/2	q_6
7	0.088	0	pi/2	q_7

Fig. 5: Modified DH parameters and robot structure of the Franka Emika Robot in (a)*H-BAM* and (b)*V-BAM* configuration.

robot joint, reduces the number of identifiable base parameters by two (see section II-A.2). Thus, the parameters $l_{xR,1}$ and $l_{yR,1}$ are only identifiable in the *H-BAM* configuration (see Table II).

Validation of the Estimation Results: To validate the results, random joint trajectories are applied to robots in both *V-BAM* and *H-BAM* configurations, and the resulting torques are compared to the modeled torques based on the identified parameters of *V-BAM* and *H-BAM* for both robot configurations.

The base inertial parameters identified in the *V-BAM* configuration can only be used for the robot installed in the *V-BAM* configuration (see Fig. 3). As a result, for the *H-BAM* robot, the estimated torques deviate from the measured/simulated ones due to the two missing inertial parameters (see Fig. 4).

In contrast, the base inertial parameters identified in the *H-BAM* configuration can be used to model the dynamics in any new robot mounting configuration. The estimated torques are in agreement with the measured/simulated torques for both *V-BAM* and *H-BAM* configurations (see Fig. 3 and 4). This result supports the hypothesis that the identified base parameters in the *H-BAM* configuration represent a more generalized base parameter set.

B. Real Robot Experiment: 7-DOF Franka Emika Robot

The base inertial parameters of a Franka Emika Robot mounted in *H-BAM* configuration are identified in a real robot experiment. The results demonstrate that these parameters can be generalized and used to accurately model the dynamics of both *H-BAM* and *V-BAM* mounting configurations of a Franka Emika Robot.

Robot Description: Fig. 5 shows the kinematic parameters of the 7-DOF manipulator. Each joint is equipped with a torque sensor and an encoder. The ISO-graded payload capacity of each arm is 3kg (without the end effector) in the worst configuration, with a total weight of approximately 18kg.

Optimal Excitation Trajectories: A normalized condition number of 43.0 is achieved with the excitation trajectories based on finite Fourier series (see Equation (11)). Before running the trajectories on the real robot, they are first simulated in *Matlab* to visualize and exclude any possible collision with the environment or the robot itself (see Fig. 6).

Estimation of Base Inertia Parameters: The identified robot base inertial parameters in *H-BAM* configuration are shown in Table III. The total number of identifiable generalized base parameters of the Franka Emika Robot is 59.

Validation of the Estimation Results: To validate the identified parameters, we generated and applied five random reference trajectories to the Franka Emika Robot in both the *H-BAM* and *V-BAM* configurations. The torques modeled with the estimated generalized robot base parameters agree with the measured joint torques for both mounting configurations (see Fig. 7 and 8). The root-mean-square (RMS) error

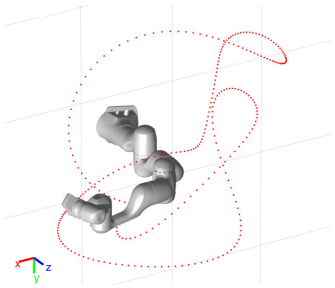

Fig. 6: Simulation of the Cartesian position of the end-effector during the optimized robot excitation.

Par.	Val.	Par.	Val.	Par.	Val.
$L_{xxR,1}$	−0.0522	$L_{yzR,4}$	0.0053	$L_{xzR,7}$	0.0033
$l_{xR,1}$	0.0125	$L_{zzR,4}$	0.6490	$L_{yzR,7}$	0.0006
$l_{yR,1}$	−0.0066	$l_{xR,4}$	−0.5050	$L_{zzR,7}$	−0.0050
$L_{xxR,2}$	1.0360	$l_{yR,4}$	1.7403	$l_{xR,7}$	0.0025
$L_{xyR,2}$	−0.0139	$L_{xxR,5}$	0.0242	$l_{yR,7}$	0.0029
$L_{xzR,2}$	0.0466	$L_{xyR,5}$	0.0007	$f_{vR,1}$	0.0105
$L_{yzR,2}$	−0.0214	$L_{xzR,5}$	−0.0089	$f_{vR,2}$	−0.0162
$L_{zzR,2}$	0.9890	$L_{yzR,5}$	−0.0124	$f_{vR,3}$	−0.0558
$l_{xR,2}$	−0.0711	$L_{zzR,5}$	0.0060	$f_{vR,4}$	0.0524
$l_{yR,2}$	−3.1936	$l_{xR,5}$	−0.0023	$f_{vR,5}$	0.1069
$L_{xxR,3}$	−0.0087	$l_{yR,5}$	0.0801	$f_{vR,6}$	0.0398
$L_{xyR,3}$	0.0030	$L_{xxR,6}$	−0.0134	$f_{vR,7}$	0.0371
$L_{xzR,3}$	0.0146	$L_{xyR,6}$	0.0024	$f_{cR,1}$	0.5182
$L_{yzR,3}$	−0.0055	$L_{xzR,6}$	−0.0018	$f_{cR,2}$	0.2830
$L_{zzR,3}$	0.1226	$L_{yzR,6}$	0.0056	$f_{cR,3}$	0.3255
$l_{xR,3}$	0.7541	$L_{zzR,6}$	0.0226	$f_{cR,4}$	0.1604
$l_{yR,3}$	−0.0001	$l_{xR,6}$	0.1615	$f_{cR,5}$	0.2937
$L_{xxR,4}$	0.5458	$l_{yR,6}$	−0.0683	$f_{cR,6}$	0.3898
$L_{xyR,4}$	0.1580	$L_{xxR,7}$	−0.0064	$f_{cR,7}$	0.1894
$L_{xzR,4}$	0.0041	$L_{xyR,7}$	0.0015		

TABLE III: Identified generalized base inertial parameters of a 7-DOF Franka Emika Robot in *H-BAM* configuration

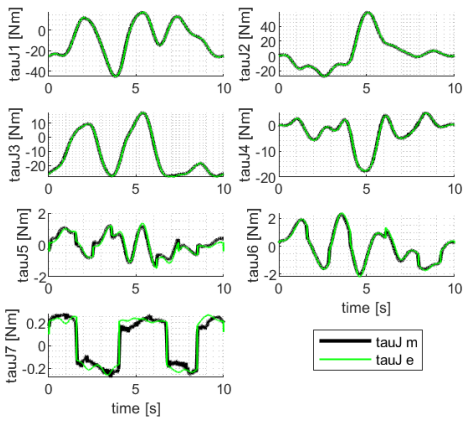

Fig. 7: Validation trajectory $traj3$ on a *H-BAM* Franka Emika Robot: Measured joint torques $tauj\ m$ versus estimated joint torques $tauj\ e$ based on the identified base inertial parameters in *H-BAM* configuration.

of all reference trajectories is shown in Tables IV and V.

Joint i	RMS [Nm] traj1	RMS [Nm] traj2	RMS [Nm] traj3	RMS [Nm] traj4	RMS [Nm] traj5
1	0.25	0.35	0.24	0.35	0.25
2	0.27	0.34	0.27	0.21	0.21
3	0.19	0.26	0.27	0.33	0.32
4	0.14	0.11	0.11	0.13	0.11
5	0.16	0.15	0.14	0.15	0.17
6	0.13	0.10	0.12	0.12	0.12
7	0.06	0.06	0.06	0.05	0.06
Mean	0.17	0.20	0.17	0.19	0.18

TABLE IV: RMS error between the measured and the estimated torques of five random reference trajectories applied on a *H-BAM* robot configuration.

Overall, our results confirmed our hypothesis that the base

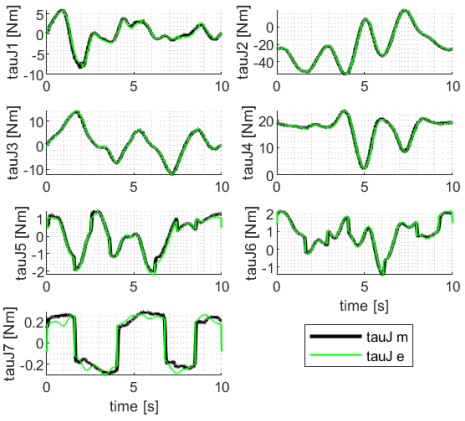

Fig. 8: Validation trajectory $traj3$ on a *V-BAM* Franka Emika Robot: Measured joint torques $tauj\ m$ versus estimated joint torques $tauj\ e$ based on the identified base inertial parameters in *H-BAM* configuration.

Joint i	RMS [Nm] traj1	RMS [Nm] traj2	RMS [Nm] traj3	RMS [Nm] traj4	RMS [Nm] traj5
1	0.21	0.30	0.28	0.30	0.29
2	0.44	0.34	0.34	0.35	0.41
3	0.16	0.21	0.17	0.16	0.13
4	0.14	0.14	0.14	0.11	0.14
5	0.18	0.17	0.14	0.16	0.20
6	0.12	0.11	0.12	0.10	0.12
7	0.06	0.07	0.06	0.05	0.07
Mean	0.19	0.19	0.18	0.18	0.19

TABLE V: RMS error between the measured and the estimated torques of five random reference trajectories applied on a *V-BAM* robot configuration.

inertial parameters identified in the *H-BAM* configuration are more generic and can be used to model the manipulator's dynamics in any new robot mounting configuration that was not used during the identification procedure, such as the *V-BAM* configuration.

IV. DISCUSSION AND CONCLUSION

The simulation results demonstrate that the inertial parameters of a robot mounted in *H-BAM* configuration can be applied to a robot mounted in *V-BAM* configuration, but not the other way around. Optimal excitation trajectories were used to identify the generalized base inertial parameters of a Franka Emika Robot mounted in *H-BAM* configuration, and it was shown that the identified parameters accurately estimate joint torques in both *H-BAM* and *V-BAM* configurations. This paper is the first to address the base inertial parameter identification problem of robotic manipulators by proposing a *GBS* that can be used for any new static robot mounting configuration.

ACKNOWLEDGEMENTS

We gratefully acknowledge the funding of the Lighthouse Initiative Geriatronics by StMWi Bayern (Project X, grant no. IUK-1807-0007// IUK582/001) and LongLeif GaPa gGmbH (Project Y). The authors acknowledge the financial support by the Federal Ministry of Education and Research of Germany (BMBF) in the program of "Souverän. Digital. Vernetzt." Joint project 6G-life, project identification number 16KISK002.

S. Haddadin has a potential conflict of interest as a shareholder of Franka Emika GmbH.

REFERENCES

[1] M. Gautier, "Dynamic identification of robots with power model," in *Proceedings of International Conference on Robotics and Automation*, vol. 3, 1997, pp. 1922–1927 vol.3.

[2] W. Khalil, F. Bennis, and M. Gautier, "Calculation of the minimum inertial parameters of tree structure robots," in *Advanced Robotics: 1989*. Springer, 1989, pp. 189–201.

[3] J. Jovic, A. Escande, K. Ayusawa, E. Yoshida, A. Kheddar, and G. Venture, "Humanoid and human inertia parameter identification using hierarchical optimization," *IEEE Transactions on Robotics*, vol. 32, no. 3, pp. 726–735, 2016.

[4] Y. Ogawa, G. Venture, and C. Ott, "Dynamic parameters identification of a humanoid robot using joint torque sensors and/or contact forces," in *2014 IEEE-RAS International Conference on Humanoid Robots*, 2014, pp. 457–462.

[5] M. Schappler, J. Vorndamme, A. Todtheide, D. C. Conner, O. von Stryk, and S. Haddadin, "Modeling, identification and joint impedance control of the atlas arms," in *2015 IEEE-RAS 15th International Conference on Humanoid Robots (Humanoids)*, 2015, pp. 1052–1059.

[6] J. Hollerbach, W. Khalil, and M. Gautier, *Model Identification*. Berlin, Heidelberg: Springer Berlin Heidelberg, 2008, pp. 321–344. [Online]. Available: https://doi.org/10.1007/978-3-540-30301-5_15

[7] A. Janot, P.-O. Vandanjon, and M. Gautier, "A generic instrumental variable approach for industrial robot identification," *IEEE Transactions on Control Systems Technology*, vol. 22, no. 1, pp. 132–145, 2014.

[8] C. Gaz, M. Cognetti, A. Oliva, P. Robuffo Giordano, and A. De Luca, "Dynamic identification of the franka emika panda robot with retrieval of feasible parameters using penalty-based optimization," *IEEE Robotics and Automation Letters*, vol. 4, no. 4, pp. 4147–4154, 2019.

[9] A. Jubien, M. Gautier, and A. Janot, "Dynamic identification of the kuka lightweight robot: Comparison between actual and confidential kuka's parameters," in *2014 IEEE/ASME International Conference on Advanced Intelligent Mechatronics*, 2014, pp. 483–488.

[10] A. Albu-Schaffer, W. Bertleff, B. Rebele, B. Schafer, K. Landzettel, and G. Hirzinger, "Rokviss - robotics component verification on iss current experimental results on parameter identification," in *Proceedings 2006 IEEE International Conference on Robotics and Automation, 2006. ICRA 2006.*, 2006, pp. 3879–3885.

[11] B. Siciliano and O. Khatib, *Springer Handbook of Robotics*. Berlin, Heidelberg: Springer-Verlag, 2007.

[12] W. Rackl, R. Lampariello, and G. Hirzinger, "Robot excitation trajectories for dynamic parameter estimation using optimized b-splines," in *2012 IEEE international conference on robotics and automation*. IEEE, 2012, pp. 2042–2047.

[13] J. Swevers, C. Ganseman, D. B. Tukel, J. De Schutter, and H. Van Brussel, "Optimal robot excitation and identification," *IEEE transactions on robotics and automation*, vol. 13, no. 5, pp. 730–740, 1997.

[14] Y. R. Stürz, L. M. Affolter, and R. S. Smith, "Parameter identification of the kuka lbr iiwa robot including constraints on physical feasibility," *IFAC-PapersOnLine*, vol. 50, no. 1, pp. 6863–6868, 2017.

[15] M. Tröbinger, C. Jähne, Z. Qu, J. Elsner, A. Reindl, S. Getz, T. Goll, B. Loinger, T. Loibl, C. Kugler *et al.*, "Introducing garmi-a service robotics platform to support the elderly at home: design philosophy, system overview and first results," *IEEE Robotics and Automation Letters*, vol. 6, no. 3, pp. 5857–5864, 2021.

[16] S. Haddadin, S. Parusel, L. Johannsmeier, S. Golz, S. Gabl, F. Walch, M. Sabaghian, C. Jaehne, L. Hausperger, and S. Haddadin, "The franka emika robot: A reference platform for robotics research and education," *IEEE Robotics Automation Magazine*, pp. 2–20, 2022.

[17] D. Jung, H. Do, T. Choi, J. Park, and J. Cheong, "Robust Parameter Estimation of Robot Manipulators Using Torque Separation Technique," *IEEE Access*, vol. 9, pp. 150 443–150 458, 2021.

[18] S. Huang, J. Chen, J. Zhang, Z. Zhu, H. Zhou, F. Li, and X. Zhou, "Robust estimation for an extended dynamic parameter set of serial manipulators and unmodeled dynamics compensation," *IEEE/ASME Transactions on Mechatronics*, vol. 27, no. 2, pp. 962–973, 2021.

[19] K.-J. Park, "Fourier-based optimal excitation trajectories for the dynamic identification of robots," *Robotica*, vol. 24, no. 5, pp. 625–633, 2006.

[20] M. Gautier, A. Janot, and P.-O. Vandanjon, "A new closed-loop output error method for parameter identification of robot dynamics," *IEEE Transactions on Control Systems Technology*, vol. 21, no. 2, pp. 428–444, 2012.